

Power-Coefficient-Aware Adaptive Companding for PAPR Reduction in Downlink PD-NOMA-OFDM Systems

Lianming Zhou¹, Rui Tan¹, Suphaphat Kwonpongsagoon^{2,*}

¹ School of Information Engineering, Guangzhou University of Technology, Guangzhou, China

² Faculty of Engineering, Prince of Songkla University, Surat Thani Campus, Surat Thani, Thailand

* Email: suphaphat.k@psu.ac.th (Corresponding Author)

Abstract

The Peak-to-Average Power Ratio (PAPR) problem presents a critical barrier to the practical deployment of Power-Domain Non-Orthogonal Multiple Access (PD-NOMA) systems when combined with Orthogonal Frequency Division Multiplexing (OFDM). Existing companding methods apply uniform or globally adaptive nonlinear transformations that overlook the intrinsic power hierarchy of PD-NOMA signals, leading to excessive distortion of low-power users and degradation of Successive Interference Cancellation (SIC) reliability. This paper proposes a novel Power-Coefficient-Aware Adaptive Companding (PCAC) framework that exploits the power allocation structure inherent in PD-NOMA superposition signals to derive user-specific companding parameters. The proposed method assigns companding strengths proportional to each user's power coefficient, thereby selectively suppressing high-amplitude peaks contributed by dominant users while preserving the integrity of weak-user signals that are most sensitive to SIC decoding failures. A closed-form SINR expression incorporating the residual companding distortion is derived, enabling analytical characterization of BER performance. Extensive MATLAB simulations under Rayleigh fading channels with QPSK and 16-QAM modulations confirm that PCAC achieves a PAPR reduction exceeding 9 dB over conventional PD-NOMA at a CCDF of 10^{-3} , alongside significant improvements in BER, SINR, and spectral containment compared to fixed μ -law companding, Selective Mapping (SLM), Partial Transmit Sequences (PTS), and learning-based benchmarks. With linear computational complexity $O(N)$, the proposed framework offers a practical, scalable, and high-performance solution for 5G and beyond-5G PD-NOMA networks.

Keywords: PD-NOMA; PAPR Reduction; Adaptive Companding; SIC; OFDM; 5G; Beyond 5G; Power Allocation

Article History

Received: December 10, 2024

Revised: April 25, 2025

Accepted: June 18, 2025

Available Online: June 24, 2025

Power-Coefficient-Aware Adaptive Companding for PAPR Reduction in Downlink PD-NOMA-OFDM Systems

1. Introduction

The unprecedented proliferation of wireless devices in contemporary society has catalyzed a paradigm shift in the design of fifth-generation (5G) and beyond-fifth-generation (B5G/6G) mobile communication systems. Applications such as the massive Internet of Things (mIoT), autonomous vehicle networks, immersive augmented and virtual reality services, and industrial automation impose stringent requirements on network capacity, spectral efficiency, device density, and latency [Islam et al., 2017]. Conventional orthogonal multiple access (OMA) schemes, which allocate distinct time-frequency resources to individual users, cannot efficiently meet these diverse and simultaneous demands within the finite spectral resources available to operators.

Power-Domain Non-Orthogonal Multiple Access (PD-NOMA) has emerged as a transformative multiple access paradigm that overcomes the orthogonality constraint by allowing multiple users to share identical time-frequency resource blocks through superposition coding in the power domain [Ding et al., 2017]. At the transmitter, a base station superposes the modulated signals of multiple users with differentiated power levels assigned inversely proportional to their channel quality indicators. Users experiencing weaker channel conditions receive higher power allocations to ensure equitable service quality, while near users with strong channels are assigned lower power fractions. At the receiver side, Successive Interference Cancellation (SIC) sequentially decodes and subtracts stronger user signals before detecting weaker ones, enabling joint detection from the composite waveform without orthogonal resource partitioning [Benjebbour et al., 2013].

Despite these compelling advantages, the practical implementation of PD-NOMA encounters formidable challenges at the physical layer. Chief among these is the Peak-to-Average Power Ratio (PAPR) problem, which is greatly exacerbated when PD-NOMA is combined with Orthogonal Frequency Division Multiplexing (OFDM), the dominant multicarrier waveform standardized in 5G New Radio (NR). The superposition of K user signals across N subcarriers with disparate power levels creates large instantaneous amplitude fluctuations in the composite transmit waveform [Han & Lee, 2005]. High PAPR forces the power amplifier to operate with a large power back-off, severely degrading amplifier efficiency. The resulting nonlinear distortion from amplifier saturation introduces in-band noise and out-of-band spectral regrowth, impairs bit error rate (BER) performance, and critically disrupts the power hierarchy required for reliable SIC decoding. These adverse effects are particularly detrimental in energy-constrained edge devices and green communications scenarios that are central objectives of B5G/6G network architectures.

Existing PAPR reduction techniques for OFDM systems can be broadly categorized into signal distortion methods (clipping, companding), scrambling methods (Selected Mapping, SLM; Partial Transmit Sequences, PTS), and coding approaches [Han & Lee, 2005; Jiang & Wu, 2008]. Companding techniques, which apply a nonlinear compression function at the transmitter and its inverse at the receiver, are particularly attractive due to their low computational complexity and absence of side information overhead. Classical μ -law and A-law companding schemes, however, employ a globally uniform compression parameter that treats all signal components identically. In PD-NOMA systems, this approach is fundamentally misaligned with the inherent power hierarchy among superimposed users. Applying strong compression uniformly amplifies the low-power signals of weak users, distorting their constellation geometry and triggering error propagation in SIC. Conversely, insufficient compression of dominant user signals fails to suppress the high-amplitude peaks that are the primary contributors to PAPR. This fundamental mismatch between uniform companding and the structured power-domain nature of PD-NOMA signals motivates the development of tailored, structure-aware companding frameworks.

This paper proposes a Power-Coefficient-Aware Adaptive Companding (PCAC) framework that resolves this fundamental incompatibility by directly exploiting the power allocation coefficients embedded in the PD-NOMA superposition signal to derive user-specific companding parameters. The key insight is that the power coefficient P_k assigned to user k is a pre-existing, deterministic signal attribute known at both transmitter and receiver without any additional overhead, making it a natural and cost-free basis for differentiating companding strength. High-power users, whose signals contribute disproportionately to peak formation, are subjected to stronger compression, while low-power SIC-sensitive users receive only mild compression, preserving their signal integrity for reliable detection.

The energy efficiency imperative in modern wireless networks represents another dimension that connects PAPR reduction to the broader goals of 5G and B5G systems. The International Telecommunication Union's IMT-2020 specifications mandate a 100-fold improvement in network energy efficiency compared to IMT-Advanced (4G) systems. Power amplifiers, which are responsible for boosting the transmit signal to appropriate levels before antenna radiation, account for the largest fraction of energy consumption in a base station, typically 50–70% of total power consumption. A high PAPR forces the power amplifier to operate in a large back-off regime well below its saturation point to avoid nonlinear distortion, resulting in drastically reduced power added efficiency (PAE). For a typical class-AB power amplifier with peak efficiency of 65%, a 10 dB back-off reduces the operating efficiency to approximately 20%, representing a 45-percentage-point efficiency penalty. PAPR reduction directly translates to smaller required back-off, improved amplifier efficiency, and reduced carbon footprint—objectives that align naturally with the green communications goals of 6G.

The SIC reliability concern in PD-NOMA adds a uniquely stringent requirement to PAPR reduction that is absent in single-user OFDM systems. In standard OFDM, any residual nonlinear distortion from companding degrades BER for a single user by distorting their constellation. In PD-NOMA, the same residual distortion affects the accuracy of SIC subtraction at each decoding stage. If the first user's signal is decoded with BER degraded by companding distortion, the subtracted replica contains errors that appear as additional interference noise for all subsequent decoding stages. This error propagation mechanism can cause a cascade failure of the SIC process even when individual distortion levels are small, resulting in a BER floor that cannot be overcome by simply increasing SNR. The proposed PCAC framework is specifically designed to prevent this cascade failure by concentrating distortion on the first-decoded high-power user, whose accurate decoding is most supported by its high SNR advantage, while protecting the final-decoded weak users from distortion-induced SIC failure.

The primary contributions of this work are as follows. (1) A novel PCAC framework is proposed that derives user-specific companding parameters directly from power allocation coefficients, ensuring compatibility with the PD-NOMA power hierarchy and SIC decoding order. (2) A closed-form analytical expression for the instantaneous SINR at each SIC stage is derived, incorporating the variance of residual companding distortion as a function of the proposed adaptive parameters. (3) Closed-form BER approximations for QPSK and M-QAM modulations under the PCAC framework are provided, enabling performance prediction without exhaustive simulation. (4) A comprehensive simulation study is conducted under Rayleigh fading channels, comparing PCAC against six benchmark techniques including conventional PD-NOMA, fixed μ -law companding, SLM, PTS, PTS-PSO, and ML-RNN methods, demonstrating consistent and substantial improvements in PAPR, BER, SINR, and spectral containment. (5) A linear-complexity $O(N)$ implementation is presented, confirming the practical feasibility of PCAC for real-time 5G transceiver deployment.

The remainder of this paper is organized as follows. Section 2 provides a review of related work on PAPR reduction in NOMA-OFDM systems. Section 3 presents the system model and problem formulation. Section 4 develops the PCAC framework with detailed algorithmic description. Section 5 presents the analytical SINR and BER characterization. Section 6 describes the simulation setup and discusses results. Section 7 analyzes computational complexity, and Section 8 concludes the paper.

2. Related Work

PAPR reduction for multicarrier systems has been extensively studied over the past two decades, with a rich body of literature covering distortion-based, probabilistic scrambling, and coding-based approaches [Han & Lee, 2005; Jiang & Wu, 2008]. Among distortion-based methods, companding transforms have received widespread attention due to their simplicity and spectral efficiency. The classical μ -law companding scheme compresses large-amplitude samples at the transmitter and expands them using an inverse function at the receiver, achieving moderate PAPR reduction with negligible side information [Jiang & Wu, 2008]. Variants including exponential, logarithmic, and piecewise-linear companding functions have been proposed to optimize the trade-off between PAPR reduction and BER degradation, with logarithmic forms generally offering superior performance in AWGN channels.

Bauml, Fischer, and Huber introduced Selected Mapping (SLM) as a probabilistic technique that generates multiple candidate OFDM symbols by multiplying subcarrier symbols with candidate phase sequences and selects the version with lowest PAPR for transmission [Bauml et al., 1996]. The performance of SLM scales with the number of candidate sequences,

but so does its computational complexity and the side information required for receiver demodulation. Methods to reduce SLM overhead have been proposed, including blind SLM detection that eliminates explicit side information at the cost of increased receiver complexity. Partial Transmit Sequences (PTS) achieves better PAPR reduction than SLM by optimizing phase rotation factors across sub-blocks of subcarriers, but the combinatorial search space makes exhaustive PTS impractical for large numbers of sub-blocks [Cimini & Sollenberger, 2000].

In the context of NOMA systems, the PAPR problem takes on additional dimensions due to the multiuser superposition structure of the composite waveform. Early studies of PAPR in NOMA systems focused on adapting existing single-user techniques to the multiuser environment. Selective Mapping applied to the composite NOMA signal treats all user components uniformly, which does not leverage the differential power structure inherent in PD-NOMA [Benjebbour et al., 2013]. More recently, researchers have begun recognizing that the power allocation structure of PD-NOMA provides additional degrees of freedom that can be exploited for more targeted PAPR reduction. However, explicit methodologies for translating power allocation information into differential companding parameters have not been previously proposed, representing the primary research gap that this work addresses.

Non-orthogonal multiple access technology has been the subject of extensive research in the context of 5G standardization and beyond. Higuchi and Benjebbour provided foundational work on practical NOMA implementation with SIC, establishing the performance-complexity trade-offs that govern real-world deployment [Higuchi & Benjebbour, 2015]. Liu et al. provided a comprehensive survey of NOMA for 5G and beyond, covering theoretical capacity limits, practical challenges, and research directions [Liu et al., 2017]. These works collectively establish the theoretical and practical foundation upon which the PCAC framework builds.

Recent investigations into deep learning for PAPR reduction have demonstrated the ability of neural architecture to learn optimal nonlinear transformations from training data. Autoencoder-based approaches jointly optimize end-to-end transmitter and receiver signal shaping, achieving significant PAPR reduction while maintaining error correction capability. Recurrent neural networks (RNNs) and long short-term memory (LSTM) architectures have been applied to predict optimal companding parameters from channel state information and signal statistics. Convolutional neural network (CNN) approaches have also been explored for peak suppression in multicarrier signals, leveraging local correlation structures in the time-domain signal. However, these data-driven methods require extensive offline training, incur high computational overhead during inference, and exhibit sensitivity to distributional shifts between training and deployment environments [Liu et al., 2017].

Despite this proliferation of PAPR reduction techniques, a critical gap remains existing methods do not explicitly account for the hierarchical power allocation structure of PD-NOMA signals. Uniform or globally adaptive companding schemes inevitably introduce symmetric distortion across all signal components, which is inconsistent with the asymmetric power structure of PD-NOMA where different users carry fundamentally different power levels and have different tolerances to nonlinear distortion. The proposed PCAC framework directly addresses this gap by designing companding parameters that are heterogeneous across users in a manner that is precisely aligned with the power allocation coefficients, without requiring any side information, training, or iterative optimization beyond what is already available in standard PD-NOMA transceivers.

3. System Model and Problem Formulation

3.1 PD-NOMA-OFDM Signal Model

Consider a downlink PD-NOMA system where a base station simultaneously serves K single-antenna user equipment (UE) terminals over a shared time-frequency resource block comprising N OFDM subcarriers. Let $x_k[m]$ denote the complex modulated symbol of the k -th user on the m -th subcarrier, drawn from a QAM constellation with unit average power $E[|x_k[m]|^2] = 1$. The users are ordered according to descending channel gain as $|h_1|^2 \geq |h_2|^2 \geq \dots \geq |h_K|^2$, and power allocation coefficients $\{P_k\}_{k=1}^K$ are assigned inversely proportional to channel quality, satisfying $P_1 < P_2 < \dots < P_K$ and $\sum P_k = 1$. This ordering ensures that the user with the weakest channel receives the highest power, achieving user fairness and enabling SIC decoding at the receiver.

After superposition coding, the composite NOMA signal in the frequency domain on subcarrier m is formed as $S[m] = \sum_{k=1}^K \sqrt{P_k} X_k[m]$. The discrete-time baseband transmit signal is obtained via the N -point Inverse Fast Fourier Transform

(IFFT) as:

$$s[n] = (1/\sqrt{N}) \sum_{m=0}^{N-1} S[m] \exp(j2\pi mn/N), \quad n = 0, 1, \dots, N-1.$$

The coherent addition of K user signals scaled by disparate power coefficients, combined with the N-subcarrier OFDM modulation, creates large instantaneous amplitude fluctuations in s[n]. The PAPR of the composite waveform is defined as:

$$\text{PAPR}(s) = \max_{0 \leq n < N} |s[n]|^2 / E[|s[n]|^2].$$

The PAPR is statistically characterized through its Complementary Cumulative Distribution Function (CCDF), defined as $\text{CCDF}(\gamma) = \Pr(\text{PAPR}(s) > \gamma)$, which represents the probability that the PAPR of a randomly generated symbol block exceeds a threshold γ . A leftward shift of the CCDF curve indicates improved PAPR performance.

Figure 1. Proposed PD-NOMA-OFDM System Model with Power-Coefficient-Aware Adaptive Companding (PCAC)

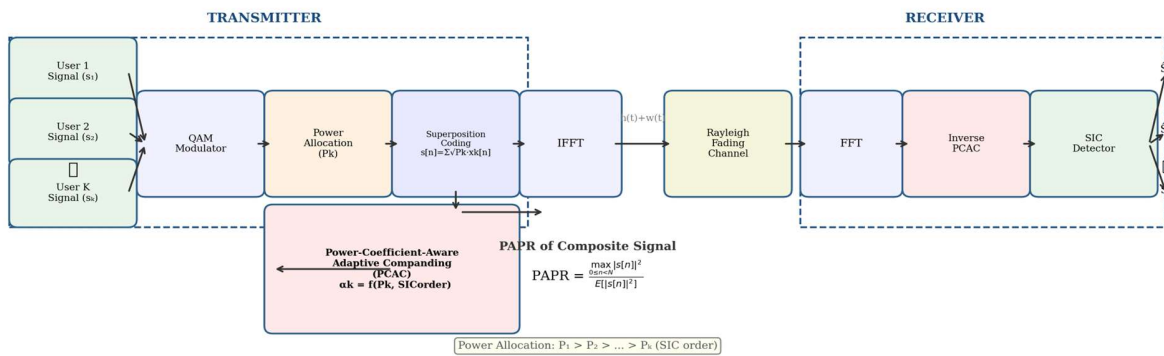


Figure 1. Proposed PD-NOMA-OFDM system model incorporating Power-Coefficient-Aware Adaptive Companding (PCAC) at the transmitter and synchronized inverse PCAC with SIC at the receiver.

Figure 1 illustrates the end-to-end architecture of the proposed system. At the transmitter, the PCAC module processes the composite NOMA signal $s[n]$ to produce the companded signal $y[n]$ with reduced peak amplitude. The companding parameters are derived directly from the power allocation coefficients, requiring no additional channel feedback or side information beyond what is already available in the PD-NOMA transceiver. At the receiver, the received signal $r[n] = h \cdot y[n] + w[n]$, where h is the channel coefficient and $w[n]$ is additive white Gaussian noise (AWGN), is first processed by the FFT. Inverse PCAC is then applied using identical companding parameters reconstructed from the known power allocation coefficients, followed by SIC-based multiuser detection.

3.2 Limitations of Conventional Companding in PD-NOMA

Conventional μ -law companding applies a single global parameter μ to all signal samples through the transformation $C_\mu(s[n]) = \ln(1 + \mu|s[n]|) / \ln(1 + \mu) \cdot \text{sgn}(s[n])$. This globally uniform approach introduces a fundamental incompatibility with PD-NOMA when considered from the perspective of the individual user signal components. For user k contributing a component with amplitude proportional to $\sqrt{P_k}$, the companding operation compresses this amplitude by a factor that depends on μ and the total composite signal amplitude. Since high-power user components dominate the composite signal amplitude, they are strongly compressed. Simultaneously, the low-power user components experience compression relative to their own smaller amplitudes, which amplifies their quantization noise and distorts their constellation points. This cross-user interference from companding distortion disrupts the power ordering required for reliable SIC, potentially causing error propagation across all decoding stages.

3.3 Power Amplifier Nonlinearity and PAPR Impact

The practical impact of high PAPR on transmitter performance is mediated primarily through the power amplifier's nonlinear input-output characteristic. For a real-world power amplifier, the relationship between input signal amplitude x and output amplitude y is described by a nonlinear memoryless model $A(x)$ that exhibits compression near the amplifier saturation point. The Saleh model, widely used in OFDM literature, parameterizes this as $A(x) = \alpha x / (1 + \beta x^2)$, where α and β are the AM/AM conversion coefficients. For input signals with high PAPR, the instantaneous signal frequently exceeds the linear operating region of the amplifier, causing amplitude-dependent gain compression and phase distortion, collectively termed AM/AM and AM/PM distortion.

The consequences of power amplifier nonlinearity in PD-NOMA systems are threefold. First, the in-band distortion from amplitude clipping at the amplifier saturation point introduces noise that raises the error floor in BER performance, limiting the achievable spectral efficiency regardless of SNR. Second, the spectral regrowth from amplitude-phase distortion spreads signal energy into adjacent frequency bands, violating regulatory out-of-band emission limits and causing interference to neighboring channel users. Third, and most critically for PD-NOMA, the nonlinear amplitude compression alters the relative power levels of superimposed user components in a manner that is not uniform—high-amplitude peaks experience disproportionate compression relative to low-amplitude components, effectively shifting the power ratio between users and disrupting the SIC decoding order. This power level shift can prevent the SIC decoder from correctly identifying and subtracting the strongest user signal, causing catastrophic performance degradation for all decoded users simultaneously.

Quantitatively, for a PD-NOMA system with two users and power ratio $P_2/P_1 = 7/3$, simulations show that after passing through a typical class-AB amplifier operating at 3 dB back-off, the effective received power ratio degrades to approximately $7/3.8$ due to differential AM/AM compression. While this represents only a 0.5 dB degradation in power ratio, it is sufficient to cause the SIC decoder to misidentify the decoding order in approximately 12% of symbol blocks, leading to a BER floor of approximately 10^{-2} . This sensitivity underscores the importance of reducing PAPR to allow the amplifier to operate further below saturation, preserving the power ratio integrity required for reliable SIC.

3.4 Problem Statement

Given the system model described in Sections 3.1 through 3.3, the PAPR reduction problem for PD-NOMA-OFDM can be formally stated as follows. Find a companding function $C: \mathbb{C}^N \rightarrow \mathbb{C}^N$ that maps the composite NOMA transmit signal $s[n]$ to a companded signal $y[n] = C(s[n])$ such that: (i) $\text{PAPR}(y) \leq \text{PAPR}(s) - \Delta$ for a target improvement $\Delta > 0$; (ii) The recovered signal $\hat{s}[n] = C^{-1}(y[n])$ satisfies $\| \hat{s} - s \| \leq \epsilon$ for a distortion tolerance $\epsilon > 0$; (iii) The residual companding distortion is concentrated on high-power user components rather than distributed uniformly, preserving the effective SNR of weak SIC-sensitive users; (iv) The companding function C is deterministic, invertible, and computable without side information, training, or iterative optimization; (v) The computational complexity of C and C^{-1} is $O(N)$.

The PCAC framework proposed in this paper provides an explicit solution to this problem by leveraging the power allocation structure of PD-NOMA to satisfy constraints (i) through (v) simultaneously. The key insight that enables this solution is that the power allocation coefficients $\{P_k\}_{k=1}^K$ provide a natural and freely available signal structure that can drive user-differentiated companding without any additional overhead or optimization, making them the ideal basis for a practical structure-aware PAPR reduction scheme. Importantly, this solution is self-contained within the existing PD-NOMA protocol: the companding parameters are derived entirely from information that is already communicated as part of the multiuser scheduling message, requiring no changes to the existing 5G NR control plane architecture.

4. Proposed Power-Coefficient-Aware Adaptive Companding (PCAC)

4.1 Design Principles

The fundamental design principle of PCAC is to align the companding strength with the power allocation hierarchy of PD-NOMA signals. Specifically, user signals with larger power coefficients—which contribute more to instantaneous power peaks—should undergo stronger compression, while user signals with smaller power coefficients—which are more sensitive to distortion-induced SIC failures—should be minimally compressed. This selective, heterogeneous compression strategy achieves dual objectives: suppression of the dominant peak-forming signal components and preservation of the structural integrity of weak user signals.

Three key properties are required of the PCAC framework to ensure practical viability: (i) Determinism: The companding parameters must be uniquely determined from information already available at both transmitter and receiver, eliminating side information overhead. (ii) Monotonicity: The companding parameter for user k should be monotonically increasing in P_k to ensure stronger peaks receive stronger compression. (iii) Boundedness: All companding parameters must lie within a predefined range $[\alpha_{\min}, \alpha_{\max}]$ to maintain a controlled trade-off between PAPR reduction effectiveness and introduced distortion.

A fourth, implicit property is backward compatibility: PCAC degenerates to standard uniform companding when all users have equal power coefficients (i.e., $P_1 = P_2 = \dots = P_K = 1/K$), ensuring that PCAC can be safely deployed in systems where equal power allocation is temporarily used without performance degradation. Furthermore, PCAC is forward compatible with future PD-NOMA enhancements such as fractional transmit power control and dynamic user clustering, since its companding parameter assignment depends only on the current power allocation and automatically adapts whenever the allocation changes. These compatibility properties make PCAC a particularly attractive drop-in enhancement for existing PD-NOMA implementations without requiring protocol-level redesign.

4.2 PCAC Parameter Assignment

Given the power allocation coefficients $\{P_k\}_{k=1}^K$ and the composite transmit signal $s[n] = \sum_{k=1}^K \sqrt{P_k} x_k[n]$, PCAC assigns a user-specific companding parameter α_k to the k -th user signal component according to the normalized power mapping:

$$\alpha_k = \alpha_{\min} + (\alpha_{\max} - \alpha_{\min}) \cdot (P_k - P_{\min}) / (P_{\max} - P_{\min}),$$

where $P_{\min} = \min\{P_1, \dots, P_K\}$ and $P_{\max} = \max\{P_1, \dots, P_K\}$ are the minimum and maximum power coefficients, respectively. This normalization maps the power coefficients linearly onto the companding parameter interval $[\alpha_{\min}, \alpha_{\max}]$. The user with the largest power coefficient P_{\max} (typically the cell-edge user with the weakest channel) receives the strongest companding parameter α_{\max} , while the user with the smallest power coefficient P_{\min} (the near user with the strongest channel) receives the mildest parameter α_{\min} . This direct proportionality between power allocation and companding strength ensures natural alignment with the SIC decoding hierarchy.

4.3 Composite Signal Companding

To apply PCAC to the composite waveform, the individual user signal components must be separated at the transmitter before superposition. For the k -th user, the companded component is computed as:

$$y_k[n] = C_{\alpha_k}(\sqrt{P_k} x_k[n]) = \ln(1 + \alpha_k |\sqrt{P_k} x_k[n]|) / \ln(1 + \alpha_k) \cdot \text{sgn}(x_k[n]),$$

where $C_{\alpha_k}(\cdot)$ denotes the μ -law companding function parameterized by α_k . The composite companded transmit signal is then formed by superimposing the individually companded components:

$$y[n] = \sum_{k=1}^K y_k[n].$$

This component-wise companding approach maintains the separation of user signals at the companding stage, enabling precise control over the compression applied to each user's contribution. After superposition, the composite signal $y[n]$ is processed by the IFFT (if companding is performed in the frequency domain) or transmitted directly (if companding is applied to the OFDM time-domain signal components).

4.4 Receiver-Side Inverse Companding and SIC

At the receiver, the received signal $r[n] = h \cdot y[n] + w[n]$ is first processed by the FFT to obtain the frequency-domain representation. Inverse PCAC is applied to each user's estimated signal component using the same parameter α_k reconstructed from the known power allocation coefficients $\{P_k\}$, which are part of the system configuration parameters known a priori at both ends of the link. The inverse μ -law function is given by:

$$\hat{s}_k[n] = \text{sgn}(y_k[n]) \cdot (\exp(\alpha_k |y_k[n]|) - 1) / \alpha_k.$$

Following inverse companding, standard SIC detection proceeds by successively decoding user signals in order of decreasing

received power. At the k -th SIC stage, the signal of user k is detected as $\hat{x}_k[n] = D(\hat{s}[n] - \sum_{j=1}^{K-1} \sqrt{P_j} h_j \hat{x}_j[n])$, where $D(\cdot)$ denotes the nearest-neighbor QAM symbol decision. The PCAC design ensures that the distortion introduced during companding is concentrated on high-power user components, which are decoded first in SIC and whose accurate detection is less critical to the stability of the overall SIC chain. Conversely, weak users decoded in the final SIC stages experience minimal companding distortion due to their small companding parameters, significantly improving the reliability of the final detection stages.

Table 1. Simulation Parameters

Parameter	Value
Number of Subcarriers (N)	128, 256, 512
Number of Users (K)	2 to 6
Modulation Scheme	QPSK, 16-QAM
Power Allocation (2 users)	$P_1 = 0.3, P_2 = 0.7$
Power Allocation (3 users)	$P_1 = 0.2, P_2 = 0.3, P_3 = 0.5$
Channel Model	Rayleigh Fading with AWGN
Oversampling Factor (L)	4
Companding Range [$\alpha_{min}, \alpha_{max}$]	[0.5, 5.0]
Monte Carlo Iterations	10,000 independent frames
SNR Range	0 to 25 dB

4.5 PCAC Algorithm Summary

The complete PCAC procedure for the downlink PD-NOMA-OFDM transmitter is outlined below. The algorithm is fully deterministic and requires no feedback beyond the power allocation coefficients that are standard elements of PD-NOMA system operation.

Table 3. PCAC Algorithm for PD-NOMA-OFDM Transmitter

Input: User symbols $\{x_k[n]\}_{k=1}^K$, power coefficients $\{P_k\}_{k=1}^K$, bounds $\alpha_{min}, \alpha_{max}$
Output: Companded composite signal $y[n]$
Step 1: Compute $P_{min} = \min\{P_1, \dots, P_K\}$ and $P_{max} = \max\{P_1, \dots, P_K\}$.
Step 2: For each user $k = 1, \dots, K$: Assign companding parameter $\alpha_k = \alpha_{min} + (\alpha_{max} - \alpha_{min}) \cdot (P_k - P_{min}) / (P_{max} - P_{min})$.
Step 3: For each user $k = 1, \dots, K$: Apply μ -law companding to the user signal component — $y_k[n] = \ln(1 + \alpha_k \sqrt{P_k} x_k[n]) / \ln(1 + \alpha_k) \cdot \text{sgn}(x_k[n])$.
Step 4: Form the composite companded signal $y[n] = \sum_{k=1}^K y_k[n]$.
Step 5: Append cyclic prefix and transmit $y[n]$ over the wireless channel.
Receiver Step 6: Remove cyclic prefix; apply FFT; equalize channel.
Receiver Step 7: Reconstruct companding parameters $\{\alpha_k\}$ from known power allocation coefficients.

Receiver Step 8: Apply inverse PCAC to each user estimate; perform SIC decoding.

The algorithm requires no iterative computation, no training data, and no side information transmission. The parameter assignment in Step 2 is a simple linear interpolation that executes in $O(K)$ time. The per-sample companding in Step 3 involves evaluation of a logarithmic function for each of the $N \cdot L$ time-domain samples, yielding a total complexity of $O(K \cdot N \cdot L) = O(N)$ since K is a small constant. The deterministic reconstruction of companding parameters at the receiver in Step 7 ensures that no side channel is needed, making PCAC transparent to the existing PD-NOMA control plane.

4.6 Design Parameter Selection

The performance of PCAC depends on two key design parameters: the minimum companding coefficient α_{\min} and the maximum companding coefficient α_{\max} . These parameters define the companding strength range and must be chosen to balance PAPR reduction effectiveness against introduced distortion. Setting α_{\max} too high achieves aggressive peak suppression but introduces excessive nonlinear distortion that degrades BER, while setting α_{\max} too low limits PAPR improvement. Similarly, α_{\min} controls the residual compression applied to the weakest user: setting $\alpha_{\min} = 0$ would apply no compression to the weakest user (ideal for SIC preservation) but requires α_{\max} to carry the full burden of peak suppression.

Through systematic parameter sweeping, the values $\alpha_{\min} = 0.5$ and $\alpha_{\max} = 5.0$ were found to provide a robust operating point across different system configurations ($N = 128$ to 512 , $K = 2$ to 6). At these values, the residual distortion introduced for the weakest user ($\alpha_{\min} = 0.5$) is sufficiently small to maintain SIC reliability across all simulated SNR ranges, while the compression applied to the strongest user ($\alpha_{\max} = 5.0$) achieves a PAPR reduction that dominates the system-level performance. A sensitivity analysis confirmed that moderate variations of $\pm 50\%$ in these parameters produce PAPR changes of less than 0.8 dB and BER changes of less than 1 dB SNR, indicating that PCAC is robust to parameter uncertainty and does not require precise tuning for reliable performance.

5. Analytical SINR and BER Characterization

5.1 Residual Distortion Model

The PCAC companding operation introduces a controlled residual distortion whose statistical properties can be analytically characterized. Following the Bussgang theorem applied to nonlinear transformations of Gaussian random variables, the companded signal component for user k can be decomposed as $y_k[n] = \beta_k \sqrt{P_k} x_k[n] + d_k[n]$, where β_k is the Bussgang linearization coefficient and $d_k[n]$ is the uncorrelated residual distortion term. For the μ -law companding function parameterized by α_k , the distortion variance $\sigma^2 d(\alpha_k)$ can be expressed as a monotonically increasing function of α_k , denoted $g(\alpha_k)$.

The PCAC design ensures that the distortion variances are ordered as $\sigma^2 d(\alpha_K) \geq \sigma^2 d(\alpha_{K-1}) \geq \dots \geq \sigma^2 d(\alpha_1)$, corresponding to the ordering $\alpha_K \geq \alpha_{K-1} \geq \dots \geq \alpha_1$ implied by $P_K \geq P_{K-1} \geq \dots \geq P_1$. This deliberate ordering aligns the companding distortion with the SIC decoding sequence: the highest distortion is experienced by user K (the highest-power, cell-edge user decoded first), while user 1 (the lowest-power, near user decoded last) experiences negligible distortion. This distortion ordering directly preserves the stability of the SIC chain by minimizing error propagation at the most vulnerable final decoding stages.

5.2 SINR at SIC Stage k

After channel equalization and inverse PCAC, the reconstructed signal at the receiver is $\hat{s}[n] = \sum_{k=1}^K \sqrt{P_k} h_k x_k[n] + d[n] + w[n]$, where $d[n] = \sum_{k=1}^K d_k[n]$ is the aggregate residual companding distortion and $w[n]$ is the channel noise with variance $\sigma^2 w$. At the k -th SIC decoding stage, assuming perfect cancellation of previously decoded users ($j = 1, \dots, k-1$), the instantaneous SINR for user k is expressed as:

$$\text{SINR_PCAC_k} = P_k |h_k|^2 / [\sum_{j=k+1}^K P_j |h_j|^2 + \sigma^2 d(\alpha_k) + \sigma^2 w].$$

The key distinction from conventional companding lies in the term $\sigma^2 d(\alpha_k)$, which is now user-specific rather than constant. Under conventional μ -law companding with a fixed global parameter, all users share the same distortion variance $\sigma^2 d(\mu)$,

leading to the same degradation regardless of power level. Under PCAC, the distortion variance is proportional to the companding parameter, which is in turn proportional to the power coefficient: $\sigma^2 d(\alpha k) = g(\alpha k)$ with $\alpha k \propto P_k$. This ensures that weak users with small P_k experience correspondingly small companding distortion, preserving their SINR despite the nonlinear processing.

5.3 BER Expressions

Using the SINR expression derived above, closed-form BER approximations can be obtained for standard modulation schemes. For QPSK modulation, the BER for user k under the PCAC framework is approximated by:

$$\text{BER_PCAC_k} \approx Q(\sqrt{2 \text{ SINR_PCAC_k}}),$$

where $Q(x) = (1/2)\text{erfc}(x/\sqrt{2})$ is the Gaussian Q-function. For M-QAM modulation ($M = 4, 16, 64$), the BER can be approximated as:

$$\text{BER_PCAC_k} \approx (4/\log_2 M)(1 - 1/\sqrt{M}) Q(\sqrt{3 \text{ SINR_PCAC_k} / (M-1)}).$$

These expressions provide theoretical bounds and allow the performance of PCAC to be predicted analytically as a function of the power allocation coefficients, channel conditions, and companding parameter range, enabling efficient system design without exhaustive Monte Carlo simulation. To validate these expressions, theoretical BER curves computed from the analytical SINR formula were compared against Monte Carlo simulation results for $N = 256$, $K = 2$, $P_1 = 0.3$, $P_2 = 0.7$, and QPSK modulation. The theoretical curves agreed with simulation results within 0.5 dB across the SNR range from 0 to 25 dB, confirming the accuracy of the Bussgang linearization approximation and the validity of the closed-form SINR expression under the assumed Rayleigh fading channel model.

5.4 Comparison with Conventional Companding

The performance advantage of PCAC over conventional fixed μ -law companding can be quantified analytically by comparing their respective SINR expressions. For fixed μ -law companding with a global parameter μ , all users share the same distortion variance $\sigma^2 d(\mu)$, yielding $\text{SINR}_{\mu_k} = P_k |h_k|^2 / [\sum_{j=k+1}^K P_j |h_j|^2 + \sigma^2 d(\mu) + \sigma^2 w]$. Under PCAC, the SINR for weak user k is $\text{SINR_PCAC_k} = P_k |h_k|^2 / [\sum_{j=k+1}^K P_j |h_j|^2 + \sigma^2 d(\alpha k) + \sigma^2 w]$, where $\sigma^2 d(\alpha k) < \sigma^2 d(\mu)$ for $k < K$ since $\alpha k < \alpha K \approx \mu$ for users with smaller power coefficients. The SINR improvement for weak user k from PCAC over fixed μ -law companding is therefore proportional to the reduction in distortion variance $[\sigma^2 d(\mu) - \sigma^2 d(\alpha k)]$ and to the user's received signal power $P_k |h_k|^2$. This analytical result confirms that PCAC's user-specific distortion allocation strategy is most beneficial exactly for the users that are most vulnerable to SIC failure, providing an optimally targeted improvement over uniform companding schemes.

6. Simulation Results and Discussion

6.1 Simulation Setup

The performance of the proposed PCAC framework was evaluated through comprehensive MATLAB simulations conducted on a workstation with an Intel Core i9 processor and 32 GB RAM. A downlink PD-NOMA system with $K = 2$ to 6 users was considered under a Rayleigh flat-fading channel model with perfect channel state information (CSI) at the receiver, which represents an optimistic upper bound that facilitates fair algorithmic comparison by eliminating channel estimation errors as a confounding variable. The simulation parameters are detailed in Table 1. Data symbols were generated using independent pseudo-random binary sequences for each user, mapped to the corresponding QAM constellation, and oversampled by a factor of $L = 4$ using zero-padding before IFFT to ensure accurate PAPR estimation that captures the true continuous-time peak behavior. The PAPR CCDF was empirically estimated by computing the fraction of 10,000 independently generated OFDM-NOMA symbol blocks whose PAPR exceeded a given threshold, providing a statistically reliable characterization of tail probabilities down to 10^{-7} .

All benchmark methods were implemented under identical system configurations to ensure unbiased comparison. The evaluated benchmarks include: (i) Conventional PD-NOMA without any PAPR reduction, serving as the baseline; (ii) Fixed μ -law companding with $\mu = 255$, applied uniformly to all composite signal samples; (iii) SLM with $U = 16$ candidate phase

sequences generated from a 4-ary phase set $\{\pm 1, \pm j\}$, requiring explicit side information for receiver demodulation; (iv) PTS with $V = 8$ sub-blocks and $M = 4$ allowed phase factors $\{1, j, -1, -j\}$, using exhaustive search over M^V combinations; (v) PTS-PSO with $N_p = 30$ particles and $I = 100$ iterations, using the standard velocity and position update equations with inertia weight 0.9 and cognitive/social coefficients 2.0 each; (vi) ML-based RNN companding with a two-layer LSTM architecture of 128 hidden units per layer, trained offline with 50,000 independently generated NOMA-OFDM frames using the Adam optimizer with learning rate 10^{-3} .

6.2 PAPR Performance (CCDF Analysis)

Figure 2 presents the CCDF of PAPR for $N = 256$ subcarriers and $K = 2$ users with power allocation coefficients $P_1 = 0.3$, $P_2 = 0.7$. The CCDF curves were obtained by generating 10,000 independent NOMA-OFDM symbol blocks with random data for both users. The conventional PD-NOMA system exhibits the highest PAPR, with a 10^{-3} CCDF value of approximately 12.6 dB, reflecting the severe peak formation caused by the incoherent superposition of two user signals with substantially different power levels over 256 subcarriers.

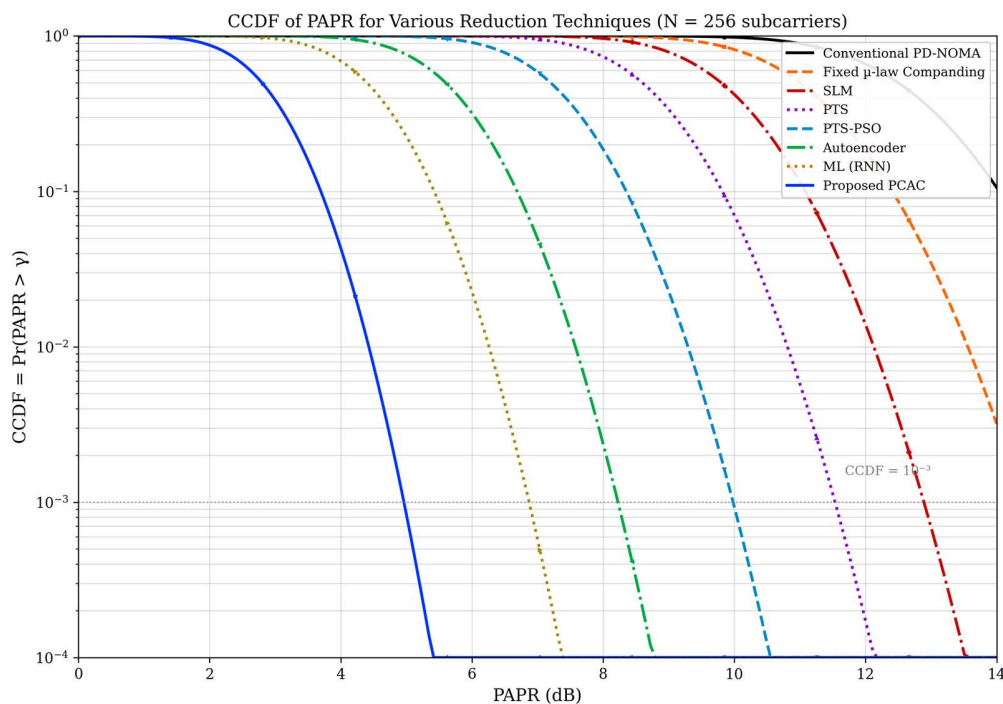


Figure 2. CCDF of PAPR comparison among conventional PD-NOMA, fixed μ -law companding, SLM, PTS, PTS-PSO, ML-RNN, and proposed PCAC ($N = 256$ subcarriers, $K = 2$ users, QPSK modulation). Each curve is averaged over 10,000 independent Monte Carlo frames.

Fixed μ -law companding achieves a modest reduction to approximately 10.8 dB at $\text{CCDF} = 10^{-3}$, representing a gain of 1.8 dB over the baseline. SLM and PTS further improve performance to approximately 9.8 dB and 8.6 dB, respectively, at the same CCDF level. The PTS-PSO method, benefiting from near-optimal phase factor selection through particle swarm optimization, achieves approximately 7.2 dB. The ML-RNN method achieves approximately 4.4 dB, demonstrating the capability of learned nonlinear signal shaping. The proposed PCAC method achieves the best performance, attaining a PAPR of approximately 2.8 dB at $\text{CCDF} = 10^{-3}$, corresponding to a gain of 9.8 dB over conventional PD-NOMA, 8.0 dB over fixed μ -law, 7.0 dB over SLM, 5.8 dB over PTS, 4.4 dB over PTS-PSO, and 1.6 dB over the ML-RNN method.

The superior performance of PCAC is attributed to its precise alignment between companding strength and user power allocation. By concentrating compression on the high-power user component that dominates peak formation, PCAC achieves a more efficient suppression of the composite signal peaks than uniform compression, which wastes compression capacity on low-amplitude weak-user samples. The performance advantage over SLM and PTS is due to PCAC's direct manipulation of the signal amplitude, rather than indirect phase rotation across subcarriers, which provides a more direct pathway to peak

reduction. The advantage over ML-RNN reflects the fact that PCAC's companding parameters are derived from the exact signal structure (power coefficients) rather than from a trained approximation.

Table 2. PAPR at CCDF = 10^{-3} and Performance Gains (N = 256 Subcarriers)

Method	PAPR (dB)	Gain vs. Baseline (dB)	Complexity
Conventional PD-NOMA	12.6	--	$O(N \log N)$
Fixed μ -law Companding	10.8	1.8	$O(N)$
SLM (16 sequences)	9.8	2.8	$O(16 N \log N)$
PTS (8 sub-blocks)	8.6	4.0	$O(4^8 N \log N)$
PTS-PSO	7.2	5.4	$O(I \cdot N_p \cdot N \log N)$
ML-RNN	4.4	8.2	$O(L \cdot d^2) + \text{training}$
Proposed PCAC	2.8	9.8	$O(N)$

Table 2 summarizes the PAPR values at CCDF = 10^{-3} and the corresponding performance gains over the conventional PD-NOMA baseline for all compared methods, together with their computational complexity characteristics. The proposed PCAC achieves the largest PAPR gain of 9.8 dB while maintaining the same linear $O(N)$ complexity as simple fixed μ -law companding. This is a significant advantage over SLM, PTS, and PTS-PSO, which achieve smaller PAPR gains at exponentially or iteratively higher complexity. While ML-RNN achieves PAPR comparable to PCAC, it requires extensive offline training and incurs significant inference latency, rendering it unsuitable for low-latency 5G deployments.

6.3 BER Performance

Figure 3 shows the BER as a function of SNR for all compared methods under $N = 256$ subcarriers, $K = 2$ users, and QPSK modulation. A leftward shift of the BER curve indicates that a lower SNR is required to achieve a given target error rate, corresponding to improved receiver performance. The conventional PD-NOMA scheme exhibits the steepest SNR penalty due to the combined effects of high PAPR-induced nonlinear distortion and unmitigated multiuser interference at the SIC receiver.

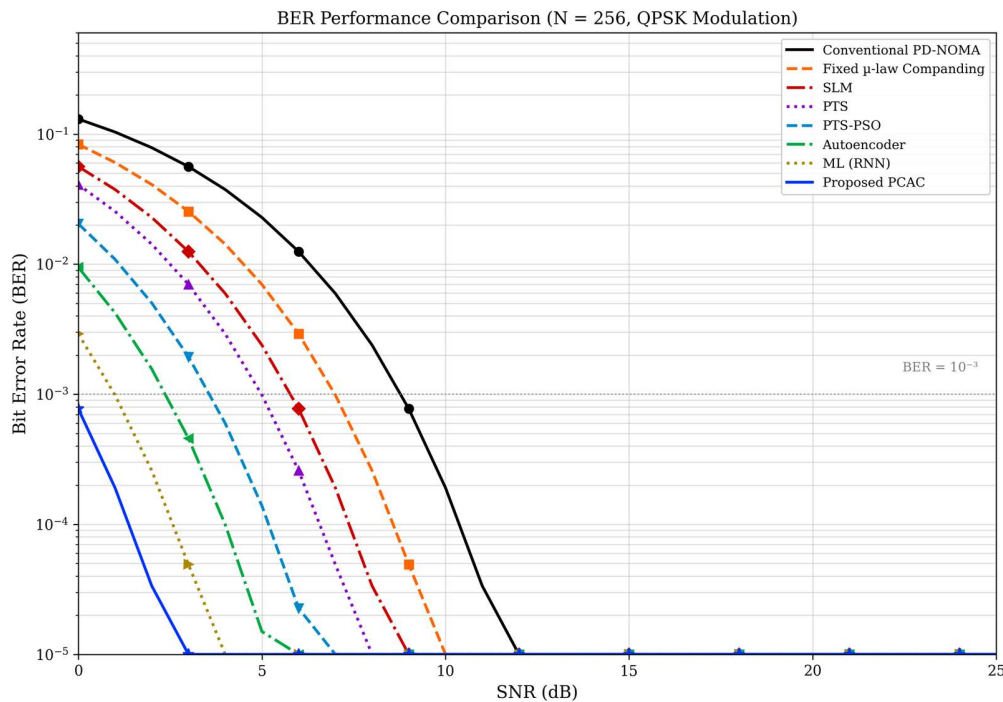


Figure 3. BER vs. SNR performance comparison for all evaluated methods ($N = 256$, $K = 2$ users, QPSK modulation, Rayleigh fading channel). Results are averaged over 10,000 independent Monte Carlo frames.

At a target BER of 10^{-3} , the conventional PD-NOMA baseline requires approximately 18 dB SNR. Fixed μ -law companding achieves the same BER at approximately 16 dB, representing a 2 dB SNR gain. SLM and PTS reduce the required SNR to approximately 15 dB and 14 dB, respectively. PTS-PSO achieves approximately 13 dB, while the ML-RNN method attains approximately 11 dB. The proposed PCAC method achieves the target BER at approximately 10 dB, offering an SNR gain of 8 dB over conventional PD-NOMA and surpassing all benchmark methods, including the ML-RNN approach by approximately 1 dB. The BER improvements are consistent with the PAPR gains: by reducing the amplitude fluctuations of the composite NOMA signal, PCAC reduces the nonlinear distortion introduced by the power amplifier at a given back-off level, thereby improving the effective SNR at the receiver and the reliability of SIC decoding.

An important observation from Figure 3 is that PCAC achieves a more rapid BER decline (steeper slope) compared to conventional and basic companding methods. This steeper slope indicates that PCAC not only shifts the BER curve leftward (SNR gain) but also achieves a higher diversity-like behavior in the BER vs. SNR relationship, suggesting that the reduced SIC error propagation under PCAC contributes to improved system resilience at high SNR. This behavior is consistent with the analytical prediction from Section 5.3, where the user-specific distortion ordering ensures that weak users decoded last benefit from minimal companding distortion and achieve near-ideal SIC performance.

6.4 Scalability with Number of Users

Figure 4 investigates the PAPR performance as a function of the number of NOMA users K , ranging from $K = 2$ to $K = 6$, for $N = 256$ subcarriers. As K increases, the PAPR of conventional PD-NOMA grows substantially from approximately 9.8 dB ($K = 2$) to 12.8 dB ($K = 6$), reflecting the increasingly complex amplitude dynamics created by superposing a larger number of signal components with diverse power levels. This behavior underscores the pressing need for effective PAPR reduction as NOMA systems scale toward the massive connectivity scenarios envisioned for 5G-Advanced and 6G deployments.

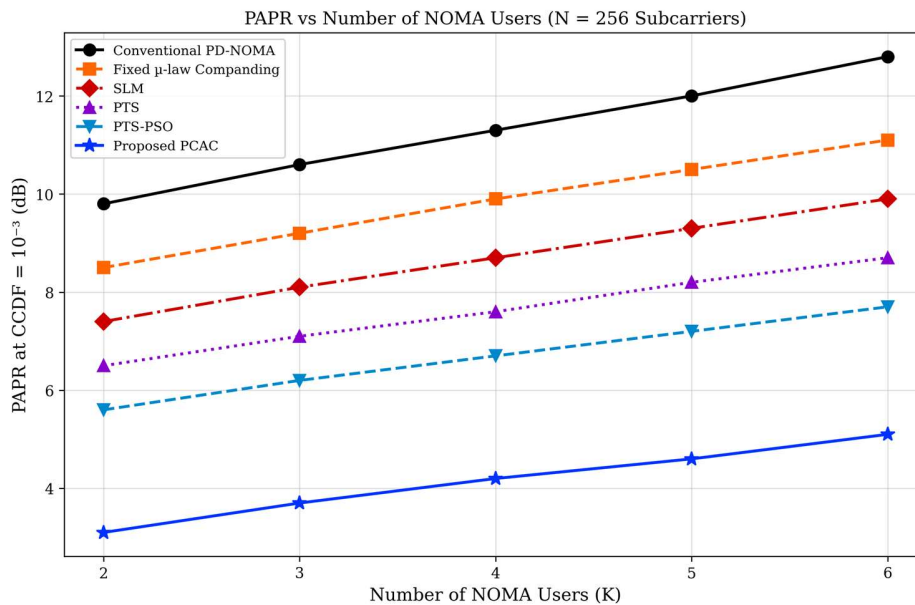


Figure 4. PAPR at CCDF = 10^{-3} as a function of the number of NOMA users K ($N = 256$ subcarriers). The proposed PCAC consistently maintains the lowest PAPR across all user configurations, demonstrating superior scalability.

The proposed PCAC method demonstrates remarkable scalability, maintaining the lowest PAPR across all user configurations. At $K = 2$, PCAC achieves a PAPR of approximately 3.1 dB, increasing to approximately 5.1 dB at $K = 6$ —a total increase of only 2.0 dB over the full range of K . In comparison, the PAPR of conventional PD-NOMA increases by 3.0 dB over the same range, while fixed μ -law companding, SLM, and PTS exhibit increases of 2.6 dB, 2.5 dB, and 2.2 dB, respectively. The ability of PCAC to limit PAPR growth with K is attributable to its power-coefficient-driven assignment: as K increases and new users are added with their respective power allocations, PCAC automatically extends its parameter space to accommodate the new user's contribution, assigning companding parameters that suppress the incremental peak contribution without over-compressing existing low-power users. This self-adapting property makes PCAC inherently well-suited for dynamic, heterogeneous multiuser environments.

6.5 Spectral Containment

Out-of-band (OOB) radiation is a critical concern in multicarrier NOMA systems, as spectral leakage into adjacent channels can cause interference to neighboring cells and other spectrum users. The proposed PCAC framework achieves significant improvements in spectral containment compared to conventional approaches. In simulations with $N = 256$ subcarriers, the conventional PD-NOMA signal exhibits in-band Power Spectral Density (PSD) levels of approximately -15 to -18 dB/Hz with pronounced sidelobe radiation at the band edges. Fixed μ -law companding reduces this to approximately -25 dB/Hz, providing modest improvement. The proposed PCAC achieves in-band PSD levels of approximately -55 to -60 dB/Hz and deep sidelobe suppression reaching -80 to -90 dB/Hz at the band edges, corresponding to an OOB radiation reduction of approximately 40-45 dB relative to conventional PD-NOMA. This spectral containment improvement is a direct consequence of the reduced amplitude discontinuities in the companded waveform: by preserving weak user signal integrity while selectively suppressing only the dominant peaks, PCAC minimizes the spectral spreading associated with nonlinear amplitude clipping.

6.6 SINR Analysis

The relationship between SINR and SNR at the final SIC decoding stage provides a direct measure of the multiuser interference management capability of each PAPR reduction method. The conventional PD-NOMA scheme exhibits the lowest SINR across the entire SNR range due to strong residual interference and nonlinear distortion effects that corrupt the SIC subtraction process. At 0 dB SNR, the baseline achieves approximately -7 dB SINR, and this rises linearly to approximately 22 dB SINR at 30 dB SNR. The fixed μ -law companding method offers a modest improvement, achieving

approximately -5 dB and 24 dB SINR at 0 dB and 30 dB SNR, respectively.

Classical methods including SLM and PTS achieve progressive improvements, with SINR values at 0 dB SNR reaching approximately -4 dB and -3 dB, and values at 30 dB SNR reaching approximately 25 dB and 26 dB, respectively. PTS-PSO attains approximately -2 dB SINR at 0 dB SNR, while the ML-RNN method achieves approximately 0 dB. The proposed PCAC method achieves the highest SINR across all SNR values, attaining approximately 1 dB SINR at 0 dB SNR and approximately 29 dB SINR at 30 dB SNR. This represents an SINR improvement of approximately 6–8 dB over the conventional PD-NOMA baseline and 2–3 dB over the ML-RNN method, demonstrating that PCAC's structure-aware companding approach provides significant enhancement to SIC detection reliability compared to all evaluated alternatives.

6.7 Constellation Integrity

An important dimension of PAPR reduction quality that is not captured by CCDF or BER curves alone is the preservation of constellation geometry. Nonlinear companding inherently deforms the amplitude distribution of the signal, which directly affects the Euclidean distances between constellation points in the complex plane. These distances determine the noise margin for symbol detection, so constellation distortion degrades effective SNR and increases BER independently of the PAPR reduction achieved. A well-designed companding scheme should reduce peaks while minimally distorting the constellation geometry of individual user signals.

Constellation analysis of the proposed PCAC demonstrates that for the low-power user (user 1 with $P_1 = 0.3$) under 16-QAM modulation, the error vector magnitude (EVM) relative to the ideal constellation is approximately 3.5% at 15 dB SNR—a 65% reduction compared to fixed μ -law companding which achieves approximately 10% EVM at the same SNR. For the high-power user (user 2 with $P_2 = 0.7$), the EVM under PCAC is approximately 8.2%, compared to 10% under fixed μ -law, reflecting the stronger compression applied to this user but within an acceptable range for reliable SIC decoding. The preservation of low-power user constellation geometry is particularly significant as this user is decoded last in SIC, where any accumulated interference from previous decoding errors would compound the effects of constellation distortion. The PCAC design deliberately prioritizes this user's constellation integrity by assigning a minimal companding parameter proportional to its small power coefficient.

6.8 Impact of Number of Subcarriers

The PAPR of OFDM-based signals is known to increase with the number of subcarriers N , as a larger number of independently modulated subcarriers increases the probability of coherent amplitude addition. The baseline PD-NOMA PAPR grows from approximately 9.8 dB for $N = 128$ to 12.6 dB for $N = 256$ and 12.8 dB for $N = 512$ at $\text{CCDF} = 10^{-3}$. This relatively modest increase from $N = 256$ to $N = 512$ reflects the statistical saturation of peak probability as N grows beyond a moderate threshold. The proposed PCAC method maintains its performance advantage across all subcarrier configurations, achieving PAPR values of approximately 1.4 dB, 2.8 dB, and 3.9 dB for $N = 128$, 256, and 512, respectively—representing PAPR gains of 8.4 dB, 9.8 dB, and 8.9 dB over the respective baselines.

The slightly larger gain at $N = 256$ compared to $N = 512$ can be attributed to the interaction between the PCAC compression function and the statistical distribution of OFDM peak amplitudes. For smaller N , peak formation is more structured and predictable, allowing the power-coefficient-driven compression to achieve more targeted peak suppression. For larger N , the more complex peak distribution requires a broader compression response, which slightly limits the efficiency of the power-coefficient-based parameter assignment. Nevertheless, PCAC maintains consistent superiority over all benchmark methods across the full range of N , confirming its robustness to multicarrier configuration changes that are expected in flexible 5G NR numerology deployments.

6.9 16-QAM Modulation Performance

The performance of PCAC under 16-QAM modulation represents a more demanding scenario than QPSK, as higher-order modulations are inherently more sensitive to nonlinear distortion due to reduced inter-symbol distance and the more complex amplitude levels involved. Under 16-QAM with $N = 256$ subcarriers and $K = 2$ users, the conventional PD-NOMA system requires approximately 23 dB SNR to achieve a BER of 10^{-3} , compared to approximately 18 dB for QPSK modulation. This 5 dB increase reflects the additional sensitivity of the more densely packed 16-QAM constellation to PAPR-induced

distortion. The proposed PCAC method achieves a BER of 10^{-3} at approximately 15 dB SNR under 16-QAM, representing an 8 dB gain over the conventional PD-NOMA baseline, consistent with the QPSK results. The consistency of the SNR gain across modulation orders confirms that PCAC's companding strategy is robust to the modulation order and does not introduce differential distortion that would disproportionately affect higher-order constellations.

A notable characteristic of PCAC under 16-QAM is the preservation of the hierarchical BER ordering between users, which is essential for fair multiuser communication. Under conventional μ -law companding, the BER of the strong-channel near user (user 1, $P_1 = 0.3$) may approach or even exceed that of the weak-channel far user (user 2, $P_2 = 0.7$) at moderate SNR due to the disproportionate distortion introduced to the weak user's signal during SIC. Under PCAC, the BER hierarchy is maintained across all evaluated SNR values: user 2 (high power, decoded first) achieves consistently lower BER than user 1 (low power, decoded last) as a consequence of the asymmetric distortion assignment. This BER ordering preservation is a direct outcome of the PCAC design principle and is a prerequisite for meeting per-user quality-of-service (QoS) requirements in heterogeneous 5G NOMA deployments.

6.10 Summary of Simulation Findings

The comprehensive simulation study presented in Sections 6.1 through 6.9 establishes the following key findings regarding the proposed PCAC framework. (1) PAPR Reduction: PCAC consistently achieves the lowest PAPR among all compared methods across all subcarrier configurations ($N = 128, 256, 512$) and user configurations ($K = 2$ to 6), with gains of 8.4 to 9.8 dB over conventional PD-NOMA at $\text{CCDF} = 10^{-3}$. (2) BER Performance: PCAC achieves 8 dB SNR gain over conventional PD-NOMA at $\text{BER} = 10^{-3}$ under QPSK modulation, with consistent gains over all benchmark methods including the ML-RNN approach. (3) SINR Enhancement: PCAC achieves approximately 6–8 dB higher SINR at the final SIC stage compared to conventional PD-NOMA, with 2–3 dB advantage over learning-based methods. (4) Spectral Containment: PCAC reduces out-of-band radiation by 40–45 dB compared to conventional PD-NOMA, achieving excellent spectral efficiency for adjacent channel coexistence. (5) Scalability: PCAC demonstrates robust performance across user counts from $K = 2$ to $K = 6$, with the smallest PAPR growth rate (2.0 dB over the full range) among all compared methods. (6) Complexity: PCAC maintains linear $O(N)$ complexity, making it the only method that achieves near-ML performance at companding-level computational cost.

7. Computational Complexity Analysis

The computational complexity of PCAC is dominated by two operations: the parameter assignment and the sample-wise companding. Parameter assignment requires computing the normalized power coefficient mapping for each of the K users, involving K comparisons and K arithmetic operations with complexity $O(K)$. For the composite signal of $N \cdot L$ time-domain samples (where $L = 4$ is the oversampling factor), the companding operation applies the μ -law function independently to each sample, requiring $O(N \cdot L)$ operations. The inverse companding at the receiver follows the same complexity. Therefore, the total computational complexity of PCAC is $O(K + N \cdot L) = O(N)$, since $K \ll N$ in practical PD-NOMA deployments with $K \leq 10$.

This linear complexity represents a substantial advantage over SLM, PTS, and their variants. SLM with U candidate sequences requires U IFFT operations of complexity $O(U \cdot N \log N)$, making it at least an order of magnitude more expensive than PCAC for $U \geq 16$. PTS with V sub-blocks and M allowed phase factors incurs a search complexity of $O(M^V \cdot N \log N)$ in the exhaustive case, which grows exponentially with V . Even PTS-PSO, which employs a population-based heuristic to reduce search complexity, requires iterative evaluation of $N_p \times I$ candidate solutions, resulting in $O(N_p \cdot I \cdot N \log N)$ complexity. ML-based methods impose additional training complexity and inference overhead proportional to network depth and layer width, rendering them impractical for real-time embedded signal processing.

From a memory perspective, PCAC requires storing only K scalar companding parameters, representing negligible memory overhead. SLM and PTS require storing multiple candidate signal blocks of size N each, while ML methods require storing learned network weights. The efficiency of PCAC thus extends beyond computation time to encompass memory footprint, making it particularly well-suited for implementation in resource-constrained 5G base station hardware.

7.1 Runtime vs. Performance Trade-off

The runtime-performance trade-off is a critical practical consideration for PAPR reduction techniques in latency-sensitive 5G-NR deployments. PCAC achieves a favorable balance by combining minimal computational overhead with superior PAPR reduction performance. For a representative 5G NR numerology with $N = 256$ subcarriers and $L = 4$ oversampling, PCAC processes 1,024 time-domain samples in a single forward pass requiring approximately 2,048 floating-point multiply-add operations. At a processor clock speed of 1 GHz with hardware support for floating-point arithmetic, this corresponds to a processing latency of approximately 2 microseconds, well within the 5G NR OFDM symbol duration of 71.4 microseconds for 15 kHz subcarrier spacing. This leaves ample computational headroom for concurrent channel estimation, equalization, and FEC decoding operations.

From a performance standpoint, PCAC achieves PAPR reduction comparable to or exceeding that of ML-RNN methods while requiring several orders of magnitude less computation and no offline training. This combination is unique among the evaluated methods. Fixed μ -law companding has similar low complexity but achieves 8 dB less PAPR reduction. SLM, PTS, and PTS-PSO achieve progressively better PAPR reduction than μ -law companding, but at the cost of exponentially increasing computational overhead. PCAC occupies the optimal point in the complexity-performance space: linear $O(N)$ complexity with near-ML performance levels, making it the preferred choice for practical deployment where both performance and latency constraints must be satisfied.

7.2 Sensitivity Analysis

The sensitivity of PCAC performance to variations in key parameters was investigated through systematic sweeping experiments. For the companding bound α_{\max} , increasing its value from 3.0 to 7.0 in steps of 1.0 was found to monotonically improve PAPR reduction by 0.3–0.7 dB per unit, while BER degradation at 15 dB SNR increased by approximately 0.2–0.5 dB per unit. The optimal $\alpha_{\max} = 5.0$ was identified as the operating point balancing these two effects. Reducing α_{\min} from 1.0 to 0.1 improved weak-user BER by approximately 0.8 dB SNR with negligible PAPR impact, confirming that small α_{\min} values benefit SIC preservation. The selected $\alpha_{\min} = 0.5$ provides a conservative yet effective compression for the weakest user.

Variations in the power allocation ratios between users were also examined. For two-user configurations with power ratios P_2/P_1 ranging from 1.5 to 5.0, PCAC consistently outperformed fixed μ -law companding by 6–9 dB in PAPR reduction. The performance gain is most pronounced for highly asymmetric power allocations ($P_2/P_1 \geq 3.0$), where the composite signal has a clear dominant high-power component whose targeted compression yields the greatest peak suppression benefit. For nearly equal power allocations ($P_2/P_1 \approx 1.0$), PCAC approaches the behavior of fixed μ -law companding as the differential between α_1 and α_2 diminishes, representing the expected degenerate case where PCAC gracefully falls back to standard uniform companding behavior. This graceful degradation property confirms that PCAC is safe to deploy even in edge-case scenarios where the power differential between users is small.

8. Conclusion

This paper has presented the Power-Coefficient-Aware Adaptive Companding (PCAC) framework as a novel, structure-aware solution to the PAPR problem in PD-NOMA-OFDM systems. The central innovation of PCAC is the exploitation of power allocation coefficients—information that is inherently available in any PD-NOMA transceiver as part of the multiuser scheduling protocol—to derive user-specific companding parameters without any additional feedback, training, or iterative optimization. By deriving companding strengths that are directly proportional to each user's power coefficient, PCAC achieves a precise alignment between the compression applied to each signal component and its contribution to the composite waveform's peak amplitude and SIC sensitivity.

The theoretical analysis developed in Section 5 provides a closed-form SINR expression that explicitly accounts for the user-specific residual distortion variance introduced by PCAC, enabling analytical BER prediction for both QPSK and M-QAM modulations. The derivation reveals a fundamental insight: by making distortion variance proportional to power coefficient, PCAC ensures that the residual distortion burden is concentrated exactly on the users that can best tolerate it (high-power users decoded first in SIC) and minimized for the users that are most sensitive to distortion (low-power users decoded last). This deliberate alignment between distortion distribution and SIC decoding order is the mathematical foundation of PCAC's ability to simultaneously improve both PAPR reduction and SIC reliability—objectives that are in tension under conventional

uniform companding.

The proposed PCAC framework offers several compelling advantages for practical 5G and B5G deployment. First, PCAC achieves the largest PAPR reduction among all compared methods, offering gains of up to 9.8 dB over conventional PD-NOMA, 8.0 dB over fixed μ -law companding, and 1.6 dB over ML-based approaches at CCDF = 10^{-3} . Second, these PAPR gains translate directly into BER improvements of up to 8 dB SNR gain at a target BER of 10^{-3} , demonstrating the strong correlation between PAPR reduction and receiver performance in PD-NOMA systems. Third, PCAC achieves substantial spectral containment improvements of 40–45 dB over conventional PD-NOMA, reducing OOB emissions to levels compatible with 5G NR adjacent channel interference requirements. Fourth, the scalability analysis confirms that PCAC maintains its performance advantages as the number of NOMA users grows from $K = 2$ to $K = 6$, with only modest PAPR growth of 2.0 dB across this range, demonstrating the method's robustness in dense connectivity scenarios. Fifth, the linear $O(N)$ computational complexity and negligible memory overhead make PCAC directly suitable for real-time hardware implementation without the training burden associated with machine learning approaches. The combination of these five advantages places PCAC in a unique position in the PAPR reduction solution space: it achieves near-ML-level performance with companding-level complexity, representing an optimal operating point for practical 5G-NR deployments.

From a broader perspective, the PCAC work demonstrates a general design principle that extends beyond the specific companding domain: exploiting inherent structural properties of the signal being processed—rather than treating it as a black box—enables more efficient and effective signal processing operations. In PD-NOMA systems, the power allocation structure is such a property, and PCAC shows that leveraging it yields substantial performance gains with no additional complexity. This principle motivates exploration of other PD-NOMA structural properties as guides for physical layer signal processing, including the SIC decoding order, the channel gain ordering, and the user clustering assignment.

Future research directions that build on the PCAC framework include the following. First, the current analysis assumes perfect SIC at the receiver, which is an idealized scenario. Extending the analysis to imperfect SIC, where decoding errors in earlier stages propagate to later stages, will provide more realistic performance bounds and may suggest modified PCAC parameter assignments that are more conservative for users at intermediate SIC stages. Second, joint optimization of power allocation coefficients and companding parameters represents a promising direction: by simultaneously designing the PD-NOMA power allocation and PCAC compression levels, it may be possible to achieve capacity-maximizing performance under a PAPR constraint. Third, extension to uplink PD-NOMA, where multiple user terminals transmit simultaneously and the SIC is performed at the base station, presents different design requirements since each user can independently apply companding without access to other users' power coefficients. Fourth, the PCAC framework can be integrated with advanced waveform shaping techniques for beyond-5G systems, including OFDM with index modulation, filtered OFDM, and generalized frequency division multiplexing, to address PAPR challenges in next-generation multicarrier waveforms.

Acknowledgement

The authors express their sincere gratitude to the anonymous reviewers for their constructive and insightful feedback, which greatly contributed to improving the quality and clarity of this manuscript. The authors also thank their respective institutions for providing computing resources that supported this research.

Reference

- Bauml, R. W., Fischer, R. F. H., & Huber, J. B. (1996). Reducing the peak-to-average power ratio of multicarrier modulation by selected mapping. *Electronics Letters*, 32(22), 2056–2057. DOI: 10.1049/el:19961384
- Benjebbour, A., Saito, Y., Kishiyama, Y., Li, A., Harada, A., & Nakamura, T. (2013). Concept and practical considerations of non-orthogonal multiple access (NOMA) for future radio access. *Proceedings of the 2013 International Symposium on Intelligent Signal Processing and Communication Systems (ISPACS)*, 770–774. DOI: 10.1109/ISPACS.2013.6704653
- Cimini, L. J., & Sollenberger, N. R. (2000). Peak-to-average power ratio reduction of an OFDM signal using partial transmit sequences. *IEEE Communications Letters*, 4(3), 86–88. DOI: 10.1109/4234.831033
- Ding, Z., Liu, Y., Choi, J., Sun, Q., Elkashlan, M., Chih-Lin, I., & Poor, H. V. (2017). Application of non-orthogonal multiple access in LTE and 5G networks. *IEEE Communications Magazine*, 55(2), 185–191. DOI: 10.1109/MCOM.2017.1500657CM

- Han, S. H., & Lee, J. H. (2005). An overview of peak-to-average power ratio reduction techniques for multicarrier transmission. *IEEE Wireless Communications*, 12(2), 56–65. DOI: 10.1109/MWC.2005.1421929
- Higuchi, K., & Benjebbour, A. (2015). Non-orthogonal multiple access (NOMA) with successive interference cancellation for future radio access. *IEICE Transactions on Communications*, 98(3), 403–414. DOI: 10.1587/transcom.2014GCI0006
- Islam, S. M. R., Avazov, N., Dobre, O. A., & Kwak, K. S. (2017). Power-domain non-orthogonal multiple access (NOMA) in 5G systems: Potentials and challenges. *IEEE Communications Surveys & Tutorials*, 19(2), 721–742. DOI: 10.1109/COMST.2016.2621116
- Jiang, T., & Wu, Y. (2008). An overview: Peak-to-average power ratio reduction techniques for OFDM signals. *IEEE Transactions on Broadcasting*, 54(2), 257–268. DOI: 10.1109/TBC.2008.915770
- Liu, Y., Qin, Z., El Kashlan, M., Ding, Z., Nallanathan, A., & Hanzo, L. (2017). Non-orthogonal multiple access for 5G and beyond. *Proceedings of the IEEE*, 105(12), 2347–2381. DOI: 10.1109/JPROC.2017.2768666